

Overmassive black holes in the $M_{\text{BH}} - \sigma$ diagram do not belong to over (dry) merged galaxies

Giulia A. D. Savorgnan^{1*}, Alister W. Graham¹

¹ *Centre for Astrophysics and Supercomputing, Swinburne University of Technology, Hawthorn, Victoria 3122, Australia.*

29 October 2014

ABSTRACT

Semi-analytical models in a Λ CDM cosmology have predicted the presence of outlying, “overmassive” black holes at the high-mass end of the (black hole mass – galaxy velocity dispersion) $M_{\text{BH}} - \sigma$ diagram (which we update here with a sample of 89 galaxies). They are a consequence of having experienced more dry mergers – thought not to increase a galaxy’s velocity dispersion – than the “main-sequence” population. Wet mergers and gas-rich processes, on the other hand, preserve the main correlation. Due to the scouring action of binary supermassive black holes, the extent of these dry mergers (since the last significant wet merger) can be traced by the ratio between the central stellar mass deficit and the black hole mass ($M_{\text{def},*}/M_{\text{BH}}$). However, in a sample of 23 galaxies with partially depleted cores, including central cluster galaxies, we show that the “overmassive” black holes are actually hosted by galaxies that appear to have undergone the lowest degree of such merging. In addition, the rotational kinematics of 37 galaxies in the $M_{\text{BH}} - \sigma$ diagram reveals that fast and slow rotators are not significantly offset from each other, also contrary to what is expected if these two populations were the product of wet and dry mergers respectively. The observations are thus not in accordance with model predictions and further investigation is required.

Key words: galaxies: evolution – galaxies: formation – galaxies: elliptical and lenticular, cD – black hole physics

1 INTRODUCTION

Our growing awareness of substructures and the actual relations within various black hole mass (M_{BH}) scaling diagrams is important because it provides us with clues into the joint evolution of black hole and host spheroid. For example, Graham (2012), Graham & Scott (2013) and Scott, Graham & Schombert (2013) have shown that the bent $M_{\text{BH}} - M_{\text{sph,dyn}}$ (spheroid dynamical mass), $M_{\text{BH}} - L_{\text{sph}}$ (spheroid luminosity) and $M_{\text{BH}} - M_{\text{sph},*}$ (spheroid stellar mass) relations reveal that black holes grow roughly quadratically with their host spheroid until the onset of dry merging, as signalled by the presence of partially depleted galaxy cores and a linear scaling at the high-mass end of these diagrams. The clever many-merger model of Peng (2007), Hirschmann et al. (2010) and Jahnke & Macciò (2011) was therefore ruled out because it required convergence along a distribution in the $M_{\text{BH}} - M_{\text{sph},*}$ diagram with a slope of unity, rather than the observed buildup (to higher masses) along the quadratic

relation.

In addition, the demographics in the $M_{\text{BH}} - \sigma$ (stellar velocity dispersion) diagram (Ferrarese & Merritt 2000; Gebhardt et al. 2000) have disclosed a tendency for barred galaxies to be offset, to higher velocity dispersions, than non-barred galaxies (Graham 2007, 2008a,b; Hu 2008; Graham & Li 2009). This may well be due to the elevated kinematics associated with bars (e.g. Graham et al. 2011; Brown et al. 2013; Hartmann et al. 2013). Speculation as to the role played by secular evolution and the possibility of “anaemic” black holes in pseudo-bulges (e.g. Graham 2008a; Hu 2008) does however still remain an intriguing possibility (Kormendy, Bender & Cornell 2011), although their current lack of an offset about the bent $M_{\text{BH}} - M_{\text{sph},*}$ relation (Graham & Scott 2013) argues against this.

An interesting suggestion for the presence of additional substructure in the $M_{\text{BH}} - \sigma$ diagram has recently been offered by Volonteri & Ciotti (2013), who investigated why central cluster galaxies tend to be outliers, hosting black holes that appear to be “overmassive” compared to expectations from their velocity dispersion. On theoretical grounds it is well known that – as a consequence of the virial theorem and the

* E-mail: gsavorgn@astro.swin.edu.au

conservation of the total energy – the mass, luminosity and size of a spheroidal galaxy increases more readily than its velocity dispersion when a galaxy undergoes (parabolic)¹ dissipationless mergers with other spheroidal galaxies (e.g. Ciotti & van Albada 2001; Nipoti, Londrillo & Ciotti 2003; Ciotti, Lanzoni & Volonteri 2007; Naab, Johansson & Ostriker 2009). In this scenario, the supermassive black hole grows through black hole binary merger events, while the galaxy velocity dispersion remains unaffected, moving the black hole/galaxy pair upward in the $M_{\text{BH}} - \sigma$ diagram. Using a combination of analytical and semi-analytical models, Volonteri & Ciotti (2013) show that central cluster galaxies can naturally become outliers in the $M_{\text{BH}} - \sigma$ diagram because they experience more mergers with spheroidal systems than any other galaxy and because these mergers are preferentially gas-poor.

Here we test this interesting idea with the latest observational data. In so doing, we update the $M_{\text{BH}} - \sigma$ diagram to include 89 galaxies now reported to have directly measured black hole masses.

2 RATIONALE

The high-mass end of the $M_{\text{BH}} - \sigma$ diagram, where a few “overmassive” outliers have now been reported to exist, is mainly populated by core-Sérsic galaxies (Graham et al. 2003; Trujillo et al. 2004), i.e. galaxies (or bulges) with partially depleted cores relative to their outer Sérsic light profile. While these galaxies are also “core galaxies”, as given by the Nuker definition (Lauer et al. 2007), it should be noted that $\sim 20\%$ of “core galaxies” are not core-Sérsic galaxies (Dullo & Graham 2014, their Appendix A.2), i.e. do not have depleted cores. Such Sérsic galaxies have no central deficit of stars. It has long been hypothesized that the presence of a partially depleted core indicates that the host galaxy has experienced one or more “dry” major mergers (Begelman, Blandford & Rees 1980). During such dissipationless mergers, the progenitor supermassive black holes are expected to sink towards the centre of the remnant, form a bound pair and release their binding energy to the surrounding stars (Milosavljević & Merritt 2001; Merritt 2013b and references therein). Indeed, the latest high-resolution observations (e.g. Sillanpää et al. 1988; Komossa et al. 2003; Maness et al. 2004; Rodriguez et al. 2006; Dotti et al. 2009; Burke-Spolaor 2011; Fabbiano et al. 2011; Ju et al. 2013; Liu et al. 2014) are providing us with compelling evidence of tight black hole binary systems. The evacuation of stars takes place within the so-called “loss-cone” of the black hole binary and has the effect of lowering the galaxy’s central stellar density (e.g. Merritt 2006a, his Figure 5; Dotti, Sesana & Decarli 2012; Colpi 2014). Upon analyzing

the central stellar kinematics of a sample of core galaxies, Thomas et al. (2014) concluded that the homology of the distribution of the orbits matches the predictions from black hole binary theoretical models, and argued that the small values of central rotation velocities favor a sequence of several minor mergers rather than a few equal-mass mergers. Subsequent to the dry merging events, AGN feedback likely prevents further star formation in the spheroids of the core-Sérsic galaxies (e.g. Ciotti, Ostriker & Proga 2010, and references therein). High-accuracy N -body simulations (Merritt 2006b) have shown that, after \mathcal{N} (equivalent) major mergers, the magnitude of the stellar mass deficit $M_{\text{def},*}$ scales as \mathcal{N} times the final mass of the relic black hole ($M_{\text{def},*} \approx 0.5\mathcal{N}M_{\text{BH}}$). This result has been used to make inferences about the galaxy merger history (e.g. Graham 2004; Ferrarese et al. 2006; Hyde et al. 2008; Dullo & Graham 2014).

If one assumes that the “overmassive” black holes belong to galaxies that have undergone a larger number of dry mergers compared to galaxies that obey the observed $M_{\text{BH}} - \sigma$ correlation (McConnell & Ma 2013; Graham & Scott 2013), it is a natural expectation that these $M_{\text{BH}} - \sigma$ outliers may also display a higher $M_{\text{def},*}/M_{\text{BH}}$ ratio when compared to the “main-sequence” population. This argument motivates our first test.

A second test can be built by looking at the kinematics of the objects that populate the $M_{\text{BH}} - \sigma$ diagram. A galaxy’s velocity dispersion remains unaffected only in the case of a dissipationless merger (with another spheroidal galaxy), whereas it accordingly increases after a dissipational (gas-rich) merger, preserving the $M_{\text{BH}} - \sigma$ correlation (Volonteri & Ciotti 2013). Wet and dry mergers may produce remnants with different kinematical structures, classified as fast (disc) and slow rotators, respectively (e.g. Emsellem et al. 2008 and references therein). Therefore, an instinctive question is whether the populations of slow and fast rotators are significantly offset from each other in the $M_{\text{BH}} - \sigma$ diagram. This will be our second test.

3 DATA

Our galaxy sample (see Table 1) consists of 89 objects for which a dynamical detection of the black hole mass and a measure of the stellar velocity dispersion have been reported in the literature. We include in our sample all the 78 objects presented in the catalog of Graham & Scott (2013), plus 10 objects taken from Rusli et al. (2013b) and 1 object from Greenhill et al. (2003). Partially depleted cores have been identified according to the same criteria used by Graham & Scott (2013). When no high-resolution image analysis was available from the literature, we inferred the presence of a partially depleted core based on the stellar velocity dispersion, σ : a galaxy is classified as core-Sérsic if $\sigma > 270 \text{ km s}^{-1}$, or as Sérsic if $\sigma \leq 166 \text{ km s}^{-1}$. This resulted in us assigning cores to just 6 galaxies, none of which were used in the following mass deficit analysis. We employ a 5% uncertainty on σ in our regression analysis.

A kinematical classification (slow/fast rotator) is available for 34 of our 89 galaxies from the ATLAS^{3D} survey

¹ In a parabolic dissipationless merger between two spheroidal galaxies, the virial velocity dispersion of the merger product cannot be larger than the maximum velocity dispersion of the progenitors. Therefore, when we say that, after such a merger, a galaxy experiences a growth of its black hole mass at a fixed velocity dispersion, we are referring to the progenitor galaxy with the highest velocity dispersion.

(Emsellem et al. 2011) and for 3 additional galaxies² from Scott et al. (2014). It is however beyond the scope of this paper to derive slow/fast rotator classifications for the remaining galaxies.

All galaxies are categorised as barred/unbarred objects according to the classification reported by Graham & Scott (2013), with the following updates. An isophotal analysis and unsharp masking of Spitzer/IRAC 3.6 μm images (Savorgnan et al. *in preparation*) has revealed the presence of a bar in the galaxies NGC 0224 (in agreement with Athanassoula & Beaton 2006; Beaton et al. 2007; Morrison et al. 2011), NGC 2974 (confirming the suggestion of Jeong et al. 2007), NGC 3031 (see also Elmegreen, Chromey & Johnson 1995; Gutiérrez et al. 2011; Erwin & Debattista 2013), NGC 3245 (see also Laurikainen et al. 2010; Gutiérrez et al. 2011), NGC 3998 (as already noted by Gutiérrez et al. 2011), NGC 4026, NGC 4388 and NGC 4736 (see also Moellenhoff, Matthias & Gerhard 1995).

Although the fast rotator galaxy NGC 1316 has been frequently classified in the literature as an elliptical merger remnant, Graham & Scott (2013) identified this object as a barred lenticular galaxy. D’Onofrio (2001) found that a single-component model cannot provide a good description of the light profile of this galaxy and de Souza, Gadotti & dos Anjos (2004) fit NGC 1316 with a bulge + exponential disc model. Sani et al. (2011) adopted a three-component model, featuring a bulge, an exponential disc and a central Gaussian (attributed to non-stellar nuclear emission). Upon an analysis of the two-dimensional velocity field obtained from the kinematics of planetary nebulae, McNeil-Moylan et al. (2012) claimed that NGC 1316 represents a transition phase from a major-merger event to a bulge-dominated galaxy like the Sombrero galaxy (M104). We find evidence for the presence of a bar in NGC 1316 from an isophotal analysis and unsharp masking of its Spitzer/IRAC 3.6 μm image (Savorgnan et al. *in preparation*), but we exclude it for now to avoid any controversy.

Central stellar mass deficits (with individual uncertainties) have been estimated for 23 core-Sérsic galaxies – with directly measured black hole masses – by Rusli et al. (2013a). Briefly, they fit the surface brightness profiles of these galaxies with a core-Sérsic model and computed the light deficit as the difference between the luminosity of the Sérsic component of the best-fitting core-Sérsic model and the luminosity of the core-Sérsic model itself. Light deficits were then converted into stellar mass deficits through dynamically-determined, individual stellar mass-to-light ratios. Rusli et al. (2013a) used galaxy distances slightly different from those adopted in this work (see Table 1), therefore we adjusted their stellar mass deficits (and uncertainties) accordingly³. Among the 23 core-Sérsic galaxies whose stellar mass deficits have been computed by Rusli et al. (2013a), 10 were also analyzed by

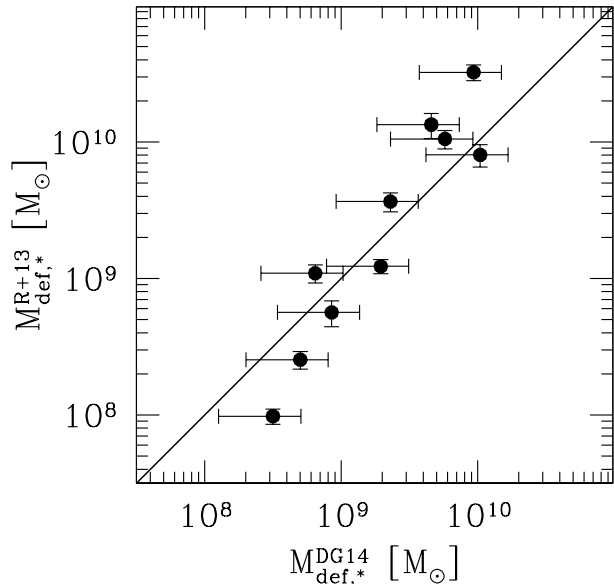


Figure 1. Comparison between the central stellar mass deficits estimated by Rusli et al. (2013a, R+13) and Dullo & Graham (2014, DG14) for ten galaxies in common. The black solid line shows the 1:1 relation. As noted in the text, the small “apparent” systematic difference is actually due to random causes.

Dullo & Graham (2014). Dullo & Graham (2014) measured light deficits with a method similar to that employed by Rusli et al. (2013a), but they converted light deficits into stellar mass deficits using stellar mass-to-light ratios derived from $V-I$ colours together with the color-age-metallicity diagram (Graham & Spitler 2009). Their stellar mass deficits are accurate to 60% (Dullo, private communication) and were rescaled according to the galaxy distances adopted here. In Figure 1 we compare these 10 common mass deficit estimates. The agreement is remarkably good, although a slight deviation from the 1:1 line can be noticed for the galaxies with the lowest or highest mass deficits, for which $M_{\text{def},*}$ reported by Dullo & Graham (2014) is larger or smaller than Rusli et al. (2013a), respectively. We checked and found that this effect actually depends in a random, i.e. non-systematic, way on the different choices to estimate the stellar mass-to-light ratios and/or their different galaxy data and modelling. We return to this point in the next Section. For these individual 10 galaxies we compute a weighted arithmetic mean of their two available stellar mass deficits.

3.1 Dark matter

The 10 black hole masses from Rusli et al. (2013b) – not to be confused with the different 10 galaxies with central mass deficits from Rusli et al. (2013a) that are in common with Dullo & Graham (2014) – were computed by taking into account the effects of dark matter. For these 10 galaxies, Rusli et al. (2013b) also published black hole masses estimated without the inclusion of dark matter halos. Among the 78 black hole masses reported by Graham & Scott (2013), only 8 had dark matter included in their derivation,

² NGC 1316, NGC 1374 and NGC 1399.

³ Mass deficits and their uncertainties from Rusli et al. (2013a) were corrected by a factor of (D/D_{prev}) . Mass deficits from Dullo & Graham (2014) were corrected by a factor of $(D/D_{\text{prev}})^2$. Here, D are the galaxy distances adopted in this work and D_{prev} are the galaxy distances used in the original works.

Table 1. Galaxy sample. *Column (1):* Galaxy names; for the 18 galaxies marked with a *, the black hole masses were estimated including in the modelling the effects of dark matter. *Column (2):* Distances. *Column (3):* Black hole masses; for the 10 measurements taken from Rusli et al. (2013b), we report in parenthesis also the measurements obtained without including in the modelling the effects of dark matter. *Column (4):* Stellar velocity dispersions. *Column (5):* References of black hole mass and velocity dispersion measurements reported here (G+03 = Greenhill et al. 2003, R+13 = Rusli et al. 2013b, GS13 = Graham & Scott 2013). *Column (6):* Presence of a partially depleted core. The question mark is used when the classification has come from the velocity dispersion criteria mentioned in Section 3. *Column (7):* Presence of a bar. *Column (8):* Central stellar mass deficits as measured by Rusli et al. (2013a). For 7 galaxies we reconstructed the “no-dark-matter” values (see Section 3.1), which are reported in parenthesis. *Column (9):* Central stellar mass deficits as measured by Dullo & Graham (2014). *Column (10):* Kinematical classification (fast/slow rotator).

Galaxy	Dist	M _{BH}	σ	Ref.	Core	Bar	M ^{R+13} _{def,*}	M ^{DG13} _{def,*}	Kinematics
(1)	(2)	[10 ⁸ M _⊙]	[km s ⁻¹]	(5)	(6)	(7)	[10 ⁸ M _⊙]	[10 ⁸ M _⊙]	(10)
A1836-BCG	158.0	39 ⁺⁴ ₋₅	309 ⁺¹⁵ ₋₁₅	GS13	yes?	no			-
A3565-BCG	40.7	11 ⁺² ₋₂	335 ⁺¹⁷ ₋₁₇	GS13	yes?	no			-
Circinus	4.0	0.017 ^{+0.004} _{-0.003}	158 ⁺⁸ ₋₈	G+03	no?	no			-
CygnusA	232.0	25 ⁺⁷ ₋₇	270 ⁺¹³ ₋₁₃	GS13	yes?	no			-
IC 1459	28.4	24 ⁺¹⁰ ₋₁₀	306 ⁺¹⁵ ₋₁₅	GS13	yes	no	16 ⁺⁷ ₋₇		-
IC 2560	40.7	0.044 ^{+0.044} _{-0.022}	144 ⁺⁷ ₋₇	GS13	no?	yes			-
M32	0.8	0.024 ^{+0.005} _{-0.005}	55 ⁺³ ₋₃	GS13	no	no			-
Milky Way	0.008	0.043 ^{+0.004} _{-0.004}	100 ⁺⁵ ₋₅	GS13	no	yes			-
NGC 0224	0.7	1.4 ^{+0.9} _{-0.3}	170 ⁺⁸ ₋₈	GS13	no	yes			-
NGC 0253	3.5	0.1 ^{+0.1} _{-0.05}	109 ⁺⁵ ₋₅	GS13	no	yes			-
NGC 0524	23.3	8.3 ^{+2.7} _{-1.3}	253 ⁺¹³ ₋₁₃	GS13	yes	no			FAST
NGC 0821	23.4	0.39 ^{+0.26} _{-0.09}	200 ⁺¹⁰ ₋₁₀	GS13	no	no			FAST
NGC 1023	11.1	0.42 ^{+0.04} _{-0.04}	204 ⁺¹⁰ ₋₁₀	GS13	no	yes			FAST
NGC 1068	15.2	0.084 ^{+0.003} _{-0.003}	165 ⁺⁸ ₋₈	GS13	no	yes			-
NGC 1194	53.9	0.66 ^{+0.03} _{-0.03}	148 ⁺⁷ ₋₇	GS13	no?	no			-
NGC 1300	20.7	0.73 ^{+0.69} _{-0.35}	229 ⁺¹¹ ₋₁₁	GS13	no	yes			-
NGC 1316	18.6	1.5 ^{+0.75} _{-0.8}	226 ⁺¹¹ ₋₁₁	GS13	no	?			FAST
NGC 1332	22.3	14.5 ⁺² ₋₂	320 ⁺¹⁶ ₋₁₆	GS13	no	no			-
NGC 1374 *	19.2	5.8 ^{+0.5} _{-0.5} (5.8)	167 ⁺⁸ ₋₈	R+13	no?	no			FAST
NGC 1399	19.4	4.7 ^{+0.6} _{-0.6}	329 ⁺¹⁶ ₋₁₆	GS13	yes	no	324 ⁺⁴² ₋₄₂	93 ⁺⁵⁶ ₋₅₆	SLOW
NGC 1407 *	28.1	45 ⁺⁴ ₋₉ (38)	276 ⁺¹⁴ ₋₁₄	R+13	yes	no	43 ⁺⁹ ₋₉ (70)		-
NGC 1550 *	51.6	37 ⁺⁴ ₋₄ (37)	270 ⁺¹³ ₋₁₃	R+13	yes	no	109 ⁺¹⁹ ₋₁₉ (117)		-
NGC 2273	28.5	0.083 ^{+0.004} _{-0.004}	145 ⁺⁷ ₋₇	GS13	no	yes			-
NGC 2549	12.3	0.14 ^{+0.02} _{-0.13}	144 ⁺⁷ ₋₇	GS13	no	yes			FAST
NGC 2778	22.3	0.15 ^{+0.09} _{-0.1}	162 ⁺⁸ ₋₈	GS13	no	yes			FAST
NGC 2787	7.3	0.4 ^{+0.04} _{-0.05}	210 ⁺¹⁰ ₋₁₀	GS13	no	yes			-
NGC 2960	81.0	0.117 ^{+0.005} _{-0.005}	166 ⁺⁸ ₋₈	GS13	no?	no			-
NGC 2974	20.9	1.7 ^{+0.2} _{-0.2}	227 ⁺¹¹ ₋₁₁	GS13	no	yes			FAST
NGC 3031	3.8	0.74 ^{+0.21} _{-0.11}	162 ⁺⁸ ₋₈	GS13	no	yes			-
NGC 3079	20.7	0.024 ^{+0.024} _{-0.012}	60 – 150	GS13	no?	yes			-
NGC 3091 *	51.3	36 ⁺² ₋₁ (9.7)	297 ⁺¹⁵ ₋₁₅	R+13	yes	no	157 ⁺³⁴ ₋₃₄ (224)		-
NGC 3115	9.4	8.8 ^{+10.0} _{-2.7}	252 ⁺¹³ ₋₁₃	GS13	no	no			-
NGC 3227	20.3	0.14 ^{+0.10} _{-0.06}	133 ⁺⁷ ₋₇	GS13	no	yes			-
NGC 3245	20.3	2 ^{+0.5} _{-0.5}	210 ⁺¹⁰ ₋₁₀	GS13	no	yes			FAST
NGC 3368	10.1	0.073 ^{+0.015} _{-0.015}	128 ⁺⁶ ₋₆	GS13	no	yes			-
NGC 3377	10.9	0.77 ^{+0.04} _{-0.06}	139 ⁺⁷ ₋₇	GS13	no	no			FAST
NGC 3379	10.3	4 ⁺¹ ₋₁	209 ⁺¹⁰ ₋₁₀	GS13	yes	no	12 ⁺¹ ₋₁	19 ⁺¹² ₋₁₂	FAST
NGC 3384	11.3	0.17 ^{+0.01} _{-0.02}	148 ⁺⁷ ₋₇	GS13	no	yes			FAST
NGC 3393	55.2	0.34 ^{+0.02} _{-0.02}	197 ⁺¹⁰ ₋₁₀	GS13	no	yes			-
NGC 3414	24.5	2.4 ^{+0.3} _{-0.3}	237 ⁺¹² ₋₁₂	GS13	no	no			SLOW
NGC 3489	11.7	0.058 ^{+0.008} _{-0.008}	105 ⁺⁵ ₋₅	GS13	no	yes			FAST
NGC 3585	19.5	3.1 ^{+1.4} _{-0.6}	206 ⁺¹⁰ ₋₁₀	GS13	no	no			-
NGC 3607	22.2	1.3 ^{+0.5} _{-0.5}	224 ⁺¹¹ ₋₁₁	GS13	no	no			FAST
NGC 3608	22.3	2 ^{+1.1} _{-0.6}	192 ⁺¹⁰ ₋₁₀	GS13	yes	no	1.0 ^{+0.1} _{-0.1}	3 ⁺² ₋₂	SLOW
NGC 3842 *	98.4	97 ⁺³⁰ ₋₂₆	270 ⁺¹³ ₋₁₃	GS13	yes	no	80 ⁺¹⁵ ₋₁₅	104 ⁺⁶³ ₋₆₃	-

Galaxy	Dist	M_{BH}	σ	Ref.	Core	Bar	$M_{\text{def},*}^{\text{R+13}}$	$M_{\text{def},*}^{\text{DG13}}$	Kinematics
(1)	Mpc	[$10^8 M_{\odot}$]	[km s^{-1}]	(5)	(6)	(7)	[$10^8 M_{\odot}$]	[$10^8 M_{\odot}$]	(10)
NGC 3998 *	13.7	$8.1^{+2}_{-1.9}$	305^{+15}_{-15}	GS13	no	yes			FAST
NGC 4026	13.2	$1.8^{+0.6}_{-0.3}$	178^{+9}_{-9}	GS13	no	yes			FAST
NGC 4151	20.0	$0.65^{+0.07}_{-0.07}$	156^{+8}_{-8}	GS13	no	yes			-
NGC 4258	7.2	$0.39^{+0.01}_{-0.01}$	134^{+7}_{-7}	GS13	no	yes			-
NGC 4261	30.8	5^{+1}_{-1}	309^{+15}_{-15}	GS13	yes	no	89^{+15}_{-15}		SLOW
NGC 4291	25.5	$3.3^{+0.9}_{-2.5}$	285^{+14}_{-14}	GS13	yes	no	11^{+2}_{-2}	6^{+4}_{-4}	-
NGC 4342	23.0	$4.5^{+2.3}_{-1.5}$	253^{+13}_{-13}	GS13	no	no			FAST
NGC 4374	17.9	$9.0^{+0.9}_{-0.8}$	296^{+15}_{-15}	GS13	yes	no	66^{+11}_{-11}		SLOW
NGC 4388	17.0	$0.075^{+0.002}_{-0.002}$	107^{+5}_{-5}	GS13	no?	yes			-
NGC 4459	15.7	$0.68^{+0.13}_{-0.13}$	178^{+9}_{-9}	GS13	no	no			FAST
NGC 4472 *	17.1	25^{+1}_{-3} (17)	300^{+15}_{-15}	R+13	yes	no	37^{+6}_{-6} (55)	23^{+14}_{-14}	SLOW
NGC 4473	15.3	$1.2^{+0.4}_{-0.9}$	179^{+9}_{-9}	GS13	no	no			FAST
NGC 4486 *	15.6	$58.0^{+3.5}_{-3.5}$	334^{+17}_{-17}	GS13	yes	no	612^{+121}_{-121}		SLOW
NGC 4486a	17.0	$0.13^{+0.08}_{-0.08}$	110^{+5}_{-5}	GS13	no	no			FAST
NGC 4552	14.9	$4.7^{+0.5}_{-0.5}$	252^{+13}_{-13}	GS13	yes	no	3^{+0}_{-0}	5^{+3}_{-3}	SLOW
NGC 4564	14.6	$0.60^{+0.03}_{-0.09}$	157^{+8}_{-8}	GS13	no	no			FAST
NGC 4594 *	9.5	$6.4^{+0.4}_{-0.4}$	297^{+15}_{-15}	GS13	yes	no			-
NGC 4596	17.0	$0.79^{+0.38}_{-0.33}$	149^{+7}_{-7}	GS13	no	yes			FAST
NGC 4621	17.8	$3.9^{+0.4}_{-0.4}$	225^{+11}_{-11}	GS13	no	no			FAST
NGC 4649 *	16.4	47^{+10}_{-10}	335^{+17}_{-17}	GS13	yes	no	105^{+16}_{-16}	58^{+35}_{-35}	FAST
NGC 4697	11.4	$1.8^{+0.2}_{-0.1}$	171^{+9}_{-9}	GS13	no	no			FAST
NGC 4736	4.4	$0.060^{+0.014}_{-0.014}$	104^{+5}_{-5}	GS13	no?	yes			-
NGC 4751 *	26.3	14^{+1}_{-1} (14)	355^{+18}_{-18}	R+13	yes?	no			-
NGC 4826	7.3	$0.016^{+0.004}_{-0.004}$	91^{+5}_{-5}	GS13	no?	no			-
NGC 4889 *	103.2	210^{+160}_{-160}	347^{+17}_{-17}	GS13	yes	no	597^{+176}_{-176}		-
NGC 4945	3.8	$0.014^{+0.014}_{-0.007}$	100^{+5}_{-5}	GS13	no?	yes			-
NGC 5077	41.2	$7.4^{+4.7}_{-3.0}$	255^{+13}_{-13}	GS13	yes	no			-
NGC 5128	3.8	$0.45^{+0.17}_{-0.10}$	120^{+6}_{-6}	GS13	no?	no			-
NGC 5328 *	64.1	47^{+19}_{-9} (0.48)	333^{+17}_{-17}	R+13	yes	no	270^{+41}_{-41} (557)		-
NGC 5516 *	58.4	33^{+3}_{-2} (32)	328^{+16}_{-16}	R+13	yes	no	135^{+31}_{-31} (145)		-
NGC 5576	24.8	$1.6^{+0.3}_{-0.4}$	171^{+9}_{-9}	GS13	no	no			SLOW
NGC 5813	31.3	$6.8^{+0.7}_{-0.7}$	239^{+12}_{-12}	GS13	yes	no	6^{+1}_{-1}	9^{+5}_{-5}	SLOW
NGC 5845	25.2	$2.6^{+0.4}_{-1.5}$	238^{+12}_{-12}	GS13	no	no			FAST
NGC 5846	24.2	11^{+1}_{-1}	237^{+12}_{-12}	GS13	yes	no	23^{+3}_{-3}		SLOW
NGC 6086 *	138.0	37^{+18}_{-11}	318^{+16}_{-16}	GS13	yes	no	76^{+18}_{-18}		-
NGC 6251	104.6	$5.9^{+2.0}_{-2.0}$	311^{+16}_{-16}	GS13	yes?	no			-
NGC 6264	146.3	$0.305^{+0.004}_{-0.004}$	159^{+8}_{-8}	GS13	no?	no			-
NGC 6323	112.4	$0.100^{+0.001}_{-0.001}$	159^{+8}_{-8}	GS13	no?	yes			-
NGC 6861 *	27.3	20^{+2}_{-2} (22)	389^{+19}_{-19}	R+13	yes?	no			-
NGC 7052	66.4	$3.7^{+2.6}_{-1.5}$	277^{+14}_{-14}	GS13	yes	no			-
NGC 7582	22.0	$0.55^{+0.26}_{-0.19}$	156^{+8}_{-8}	GS13	no	yes			-
NGC 7619 *	51.5	25^{+3}_{-8} (4.2)	292^{+15}_{-15}	R+13	yes	no	134^{+28}_{-28} (232)	46^{+27}_{-27}	-
NGC 7768 *	112.8	13^{+5}_{-4}	257^{+13}_{-13}	GS13	yes	no	25^{+5}_{-5}		-
UGC 3789	48.4	$0.108^{+0.005}_{-0.005}$	107^{+5}_{-5}	GS13	no?	yes			-

and no dark matter halo was included by Greenhill et al. (2003) in their black hole mass estimate.

The majority⁴ of the 23 stellar mass deficits from Rusli et al. (2013a) were derived from their analysis which incorporated dark matter to obtain the central mass-to-light ratios. However, Rusli et al. (2013a) did not publish the corresponding stellar mass deficits for the no-dark-matter case. Therefore,

⁴ Stellar mass deficits for IC 1459, NGC 3379, NGC 4374 and NGC 4261 were estimated by Rusli et al. (2013a) with single-component dynamical modelling, i.e. without dark matter.

the sample of 89 galaxies that we use in our analysis contains 18 black hole masses estimated with the inclusion of a dark matter halo and the 23 stellar mass deficits published by Rusli et al. (2013a).

We have already shown in Section 3 that the stellar mass deficits measured by Dullo & Graham (2014), without accounting for dark matter, are in good agreement with the Rusli et al. (2013a) estimates which accounted for dark matter. The slight disagreement observed for the lowest and highest mass deficits (see Figure 1) does not significantly affect the conclusions of our analysis. However, one could wonder whether our results change when using exclusively

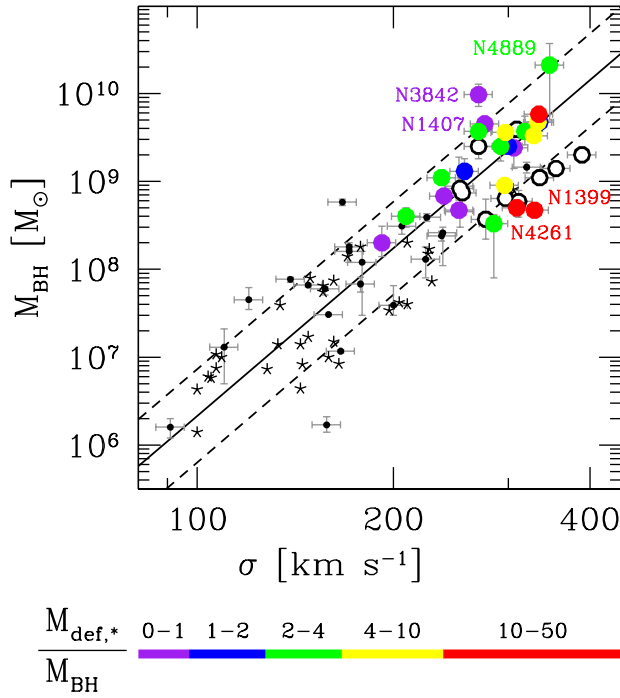


Figure 2. $M_{\text{BH}} - \sigma$ diagram for the 89 galaxies presented in Table 1. Core-Sérsic galaxies are colour coded according to their $M_{\text{def},*}/M_{\text{BH}}$ ratio. If no $M_{\text{def},*}$ estimate is available, they appear as open circles. Unbarred Sérsic galaxies are represented with (small) black dots and barred Sérsic galaxies with starred symbols. Errors bars are reported only for unbarred galaxies used to derive Equation 1. The black solid line shows the $\text{OLS}(\sigma|M_{\text{BH}})$ linear regression for all non-barred galaxies and the black dashed lines mark the associated total rms scatter ($\Delta = 0.53$) in the $\log(M_{\text{BH}})$ direction.

black hole masses and stellar mass deficits derived without the inclusion of dark matter. To address this question, we derived the no-dark-matter stellar mass deficits⁵ for 7 of the 10 galaxies whose black hole masses were measured by Rusli et al. (2013b). We repeated the analysis by (i) employing for these 7 galaxies the no-dark-matter black hole masses (published by Rusli et al. 2013b) and the no-dark-matter stellar mass deficits (derived by us), and (ii) excluding the remaining black hole masses estimated with the inclusion of dark matter. We found that none of our conclusions was affected by this change.

4 RESULTS

In Figure 2, we show the updated $M_{\text{BH}} - \sigma$ diagram for the 89 galaxies listed in Table 1. Core-Sérsic galaxies are colour coded according to their $M_{\text{def},*}/M_{\text{BH}}$ ratio (or, if no $M_{\text{def},*}$

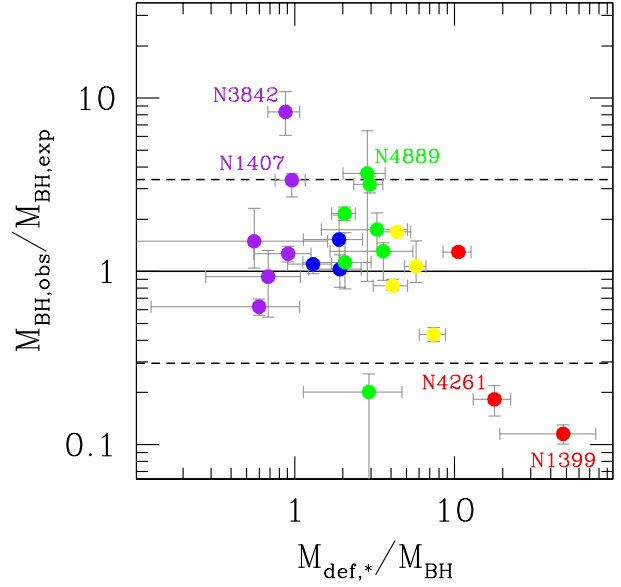


Figure 3. Vertical offset from the $M_{\text{BH}} - \sigma$ relation versus the $M_{\text{def},*}/M_{\text{BH}}$ ratio. Symbols are colour coded according to Figure 2. The vertical error bars represent the uncertainty on M_{BH} . The horizontal solid line is equivalent to a zero vertical offset from the *expected* mass ($M_{\text{BH,obs}}/M_{\text{BH,exp}} = 1$) and the horizontal dashed lines show the total rms scatter ($\Delta = 0.53$) of the $\text{OLS}(\sigma|M_{\text{BH}})$ linear regression in the $\log(M_{\text{BH}})$ direction.

estimate is available, they appear as empty symbols⁶). It is immediately evident that the “overmassive” black holes are not hosted by galaxies with a high $M_{\text{def},*}/M_{\text{BH}}$ value.

NGC 4889, NGC 3842 and NGC 1407 are the three objects with the largest positive vertical offset from the $M_{\text{BH}} - \sigma$ correlation. Contrary to expectations, these three galaxies have a small $M_{\text{def},*}/M_{\text{BH}}$ ratio, consistent with ~ 1 –2 major dry merger events (Merritt 2006b).

Remarkably, NGC 4261 and NGC 1399 – the central galaxy in the Fornax cluster – which are two of the three galaxies with $M_{\text{def},*}/M_{\text{BH}} > 10$ (red symbols in Figure 2), display a negative vertical offset from the correlation⁷. While the offset of NGC 1399 and NGC 4261 is at odds with predictions from semi-analytical models (see Section 1), their large stellar deficits might be due to the effects of a recoiling black hole (see also Dullo & Graham 2014; Lena et al. 2014). A recoiling black hole is the final product of a coalesced black hole binary after the anisotropic emission of gravitational waves, which imparts a net impulse – a kick – to the remnant black hole (Bekenstein 1973; Fitchett & Detweiler 1984; Favata, Hughes & Holz 2004; Holley-Bockelmann et al. 2008; Batcheldor et al. 2010). The kicked black hole oscillates about the centre of the newly merged galaxy with decreasing amplitude, transferring kinetic energy to the stars and thus further lowering the

⁵ The no-dark-matter stellar mass deficits were calculated as $M_{\text{def},*}^{\text{noDM}} = M_{\text{def},*}^{\text{DM}} \cdot [(M/L)^{\text{DM}}]^{-1} \cdot (M/L)^{\text{noDM}}$, where $M_{\text{def},*}^{\text{DM}}$ are the mass deficits from Rusli et al. (2013a), which had dark matter incorporated in their derivation, and $(M/L)^{\text{DM}}$ and $(M/L)^{\text{noDM}}$ are the mass-to-light ratios from Rusli et al. (2013b) estimated with and without accounting for dark matter respectively.

⁶ The 10 empty symbols refer to 6 suspected, plus 4 apparent core-Sérsic galaxies.

⁷ Although we have used the black hole mass for NGC 1399 from Gebhardt et al. (2007), we note that Houghton et al. (2006) had reported a value twice as large ($\sim 10^9 M_{\odot}$). Nevertheless, this is still too low to yield a positive offset for this galaxy in Figure 2.

core density (Redmount & Rees 1989; Merritt et al. 2004; Boylan-Kolchin, Ma & Quataert 2004). Kick-induced partially depleted cores can be as large as $M_{\text{def},*} \sim (4-5)M_{\text{BH}}$ (Gualandris & Merritt 2008) and could complicate the use of central mass deficits as a tracer of dry galaxy mergers. However, they don’t explain the low $M_{\text{def},*}/M_{\text{BH}}$ ratios observed in the “overmassive” black hole sample.

In Figure 3, we plot the vertical offset from the $M_{\text{BH}} - \sigma$ relation versus the $M_{\text{def},*}/M_{\text{BH}}$ ratio. The vertical offset is defined as $\log(M_{\text{BH,obs}}/M_{\text{BH,exp}})$, where $M_{\text{BH,obs}}$ is the *observed* black hole mass and $M_{\text{BH,exp}}$ is the black hole mass *expected* from the galaxy velocity dispersion using an $\text{OLS}(\sigma|M_{\text{BH}})$ linear regression⁸ for all non-barred⁹ galaxies:

$$\log\left(\frac{M_{\text{BH,exp}}}{M_{\odot}}\right) = (8.24 \pm 0.10) + (6.34 \pm 0.80) \times \log\left(\frac{\sigma}{200 \text{ km s}^{-1}}\right). \quad (1)$$

Clearly, there is no positive trend in Figure 3. The significance of a correlation is rejected by a Spearman’s test (Spearman’s correlation coefficient $r_s = -0.33$, likelihood of the correlation occurring by chance $P > 5\%$). We conclude that no positive correlation is observed between the vertical offset from the $M_{\text{BH}} - \sigma$ relation and the $M_{\text{def},*}/M_{\text{BH}}$ ratio. Repeating the analysis using only the Rusli et al. (2013a) mass deficits, i.e. without computing 10 weighted arithmetic means for the galaxies in common with Dullo & Graham (2014), gives the same conclusion. Similarly, the same conclusion is reached when using only the 10 Dullo & Graham (2014) derived mass deficits.

In Figure 4 we show the distribution of fast and slow rotators in the $M_{\text{BH}} - \sigma$ diagram. Our aim is to check whether the two populations are vertically offset from each other, in the sense that wet mergers can create fast rotating discs, while dry mergers can increase the black hole mass but not the velocity dispersion. Since the work of Graham (2008a,b), see also Hu (2008), we know that barred galaxies tend to be offset rightward from the $M_{\text{BH}} - \sigma$ correlation defined by non-barred galaxies. It is therefore crucial to exclude the barred galaxies from the following analysis, to avoid biasing the results. We follow Graham & Scott (2013) in using the BCES code from Akritas & Bershady (1996) to obtain four different linear regressions for both the (unbarred) fast and slow rotators. The results are shown in the first part of Table 2. Regardless of the linear regression method used, the best-fit slopes and intercepts of fast and slow rotators are consistent with each other within the 1σ uncertainty. To test the robustness of our results, we repeated the linear regression analysis excluding the most deviating data points: one fast rotator with a positive

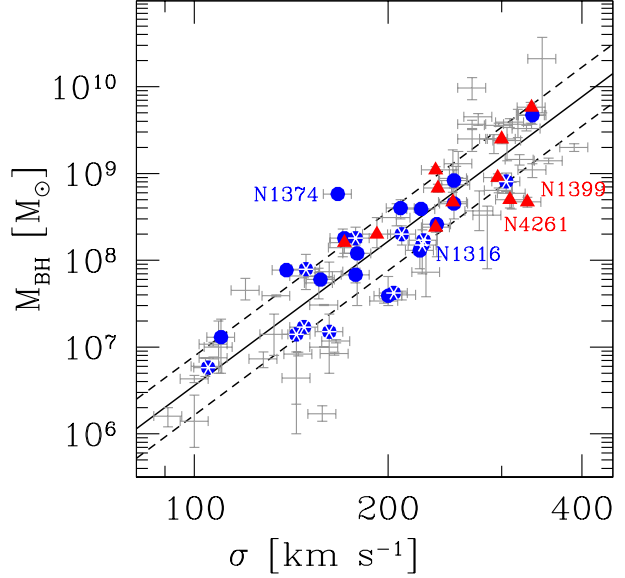


Figure 4. Fast (blue circles) and slow (red triangles) rotators in the $M_{\text{BH}} - \sigma$ diagram. Starred symbols mark barred galaxies. The black solid and dashed lines are the same as in Figure 2.

Table 2. Linear regression analysis for the populations of unbarred fast and slow rotators.

Regression	Slow rot.		Fast rot.	
	β	α	β	α
$\log[M_{\text{BH}}/M_{\odot}] = \alpha + \beta \log[\sigma/(200 \text{ km s}^{-1})]$				
OLS($M_{\text{BH}} \sigma$)	3.7 ± 1.1	8.40 ± 0.08	4.4 ± 0.6	8.33 ± 0.09
OLS(σM_{BH})	6.8 ± 1.7	8.1 ± 0.3	5.9 ± 1.0	8.3 ± 0.1
Bisector	4.8 ± 1.0	8.3 ± 0.1	5.1 ± 0.5	8.33 ± 0.09
Orthogonal	6.7 ± 1.6	8.1 ± 0.3	5.8 ± 1.0	8.3 ± 0.1
<i>Excluding NGC 1374, NGC 1399 and NGC 4261.</i>				
OLS($M_{\text{BH}} \sigma$)	5.3 ± 0.8	8.36 ± 0.09	4.7 ± 0.6	8.27 ± 0.08
OLS(σM_{BH})	6.2 ± 0.9	8.3 ± 0.1	5.4 ± 0.8	8.28 ± 0.08
Bisector	5.7 ± 0.8	8.3 ± 0.1	5.0 ± 0.6	8.27 ± 0.08
Orthogonal	6.1 ± 0.9	8.3 ± 0.1	5.4 ± 0.8	8.28 ± 0.08

vertical offset (NGC 1374) and two slow rotators with a negative vertical offset (NGC 1399 and NGC 4261). The second part of Table 2 reports the new values of the best-fit slopes and intercepts, which remain consistent with each other.

5 DISCUSSION AND CONCLUSIONS

The presence of a central, supermassive black hole, coupled with the scarcity of binary supermassive black hole systems, suggests that the progenitor black holes have coalesced in most merged galaxies. They can do this by transferring their orbital angular momentum to the stars near the centre of their host galaxy and thereby evacuating the core. If a galaxy’s $M_{\text{def},*}/M_{\text{BH}}$ ratio is a proxy

⁸ See Graham & Scott (2013, their Section 3.1) for a discussion on the choice of an ordinary least-squares (OLS) regression of the abscissa on the ordinate. Their $\text{OLS}(\sigma|M_{\text{BH}})$ linear regression for unbarred galaxies ($\log(M_{\text{BH,exp}}/M_{\odot}) = (8.22 \pm 0.05) + (5.53 \pm 0.34) \times \log(\sigma/200 \text{ km s}^{-1})$) is consistent within the over-lapping 1σ uncertainties. It is however beyond the scope of this paper to repeat the same detailed analysis presented by Graham & Scott (2013).

⁹ As noted in Section 1, barred galaxies tend to be offset from non-barred galaxies in the $M_{\text{BH}} - \sigma$ diagram.

for its equivalent number of major dry merger events since its last wet merger (e.g. Merritt 2006b), then our analysis (see Figures 2 and 3) reveals that the apparent “overmassive” outliers at the high-mass end of the $M_{\text{BH}} - \sigma$ diagram are galaxies that have undergone the lowest degree of such recent dry merging. Although a final major wet merger may contribute to their low $M_{\text{def},*}/M_{\text{BH}}$ ratio, these galaxies are among the most massive early-type galaxies in the local Universe and they reside in the central regions of galaxy clusters, where wet major mergers are unlikely to occur (e.g. Fraser-McKelvie, Brown & Pimbblet 2014) due to prior ram pressure stripping of gas from infalling galaxies (Boselli & Gavazzi 2006; Haines et al. 2013; Boselli et al. 2014a,b). That is, the “overmassive” black holes in central cluster galaxies cannot be explained by a large number of dissipationless mergers growing the black hole mass at a fixed galaxy velocity dispersion.

In addition to this, no significant offset is observed between the (unbarred) populations of fast and slow rotators in the $M_{\text{BH}} - \sigma$ diagram (see Table 2), contrary to what is expected if fast and slow rotators are, in general, the products of wet and dry mergers respectively. This is because dry mergers will increase the black hole mass, but are said not to increase the velocity dispersion. This result is also in broad agreement with the observation that the (unbarred) Sérsic and core-Sérsic galaxies follow the same $M_{\text{BH}} - \sigma$ relation (Graham & Scott 2013). Our results appear consistent with studies of luminous elliptical galaxies which have shown that the galaxy luminosity scales with the velocity dispersion (Schechter 1980; Malumuth & Kirshner 1981; von der Linden et al. 2007; Lauer et al. 2007; Bernardi et al. 2007; Liu et al. 2008), i.e. the velocity dispersion appears not to completely saturate but rather still increases with increasing galaxy luminosity, contrary to what one would predict if these galaxies were built only by dry mergers on parabolic orbits.

An alternative possibility for the central cluster galaxies may be that they experience minor dry merger events that do not bring in a massive black hole but rather stars, and nuclear star clusters, which may partly or fully refill a depleted galaxy core. However, simulations are needed to verify whether, in a Λ CDM cosmology, the extent of minor dry mergers experienced by a central cluster galaxy in late cosmic times can supply enough stellar mass ($\sim 10^9 - 10^{10} M_{\odot}$) to replenish the galaxy’s core.

Eventually, one should also consider the possibility that some of the overmassive black holes might have had their masses overestimated. Past studies have demonstrated the importance of resolving the black hole sphere-of-influence¹⁰ when measuring a black hole mass, to avoid systematic errors or even spurious detections (e.g. Ferrarese & Merritt 2000; Merritt & Ferrarese 2001a,b; Valluri, Merritt & Emsellem 2004; Ferrarese & Ford 2005). Merritt (2013a) cautions against the use of black hole mass measurements obtained from stellar-dynamical data sets. His Figure 2.5 points out that no more than three galaxies – all belonging to the Local Group – have been ob-

served with enough spatial resolution to exhibit a *prima facie* convincing Keplerian rise in their central stellar velocities. At the same time, gas kinematics can have motions not solely due to the gravitational potential of the black hole. For example, Mazzalay et al. (2014) showed that the gas dynamics in the innermost parsecs of spiral galaxies is typically far from simple circular motion. One possible example of such an overestimated black hole may be that reported by van den Bosch et al. (2012) for the galaxy NGC 1277 ($M_{\text{BH}} = 1.7 \times 10^{10} M_{\odot}$). In fact, upon re-analyzing the same data, Emsellem (2013) showed that a model with a 2 times smaller black hole mass provides an equally good fit to the observed kinematics, and emphasized the need for higher spatial resolution spectroscopic data.

ACKNOWLEDGMENTS

GS would like to acknowledge the valuable feedback provided by David Merritt and Luca Ciotti on an early version of the manuscript. GS thanks Gonzalo Díaz and Biligun Dullo for useful discussions. This research was supported by Australian Research Council funding through grants DP110103509 and FT110100263. This research has made use of the GOLDMine website (Gavazzi et al. 2003) and the NASA/IPAC Extragalactic Database (NED) which is operated by the Jet Propulsion Laboratory, California Institute of Technology, under contract with the National Aeronautics and Space Administration. We wish to thank an anonymous referee whose criticism helped improving the manuscript.

REFERENCES

- Akritas M. G., Bershadsky M. A., 1996, *ApJ*, 470, 706
- Athanassoula E., Beaton R. L., 2006, *MNRAS*, 370, 1499
- Batcheldor D., Robinson A., Axon D. J., Perlman E. S., Merritt D., 2010, *ApJ*, 717, L6
- Beaton R. L. et al., 2007, *ApJ*, 658, L91
- Begelman M. C., Blandford R. D., Rees M. J., 1980, *Nature*, 287, 307
- Bekenstein J. D., 1973, *ApJ*, 183, 657
- Bernardi M., Hyde J. B., Sheth R. K., Miller C. J., Nichol R. C., 2007, *AJ*, 133, 1741
- Boselli A., Cortese L., Boquien M., Boissier S., Catinella B., Gavazzi G., Lagos C., Saintonge A., 2014a, *A&A*, 564, A67
- Boselli A., Gavazzi G., 2006, *PASP*, 118, 517
- Boselli A. et al., 2014b, *ArXiv e-prints*
- Boylan-Kolchin M., Ma C.-P., Quataert E., 2004, *ApJ*, 613, L37
- Brown J. S., Valluri M., Shen J., Debattista V. P., 2013, *ApJ*, 778, 151
- Burke-Spolaor S., 2011, *MNRAS*, 410, 2113
- Ciotti L., Lanzoni B., Volonteri M., 2007, *ApJ*, 658, 65
- Ciotti L., Ostriker J. P., Proga D., 2010, *ApJ*, 717, 708
- Ciotti L., van Albada T. S., 2001, *ApJ*, 552, L13
- Colpi M., 2014, *Space Sci. Rev.*
- de Souza R. E., Gadotti D. A., dos Anjos S., 2004, *ApJS*, 153, 411
- D’Onofrio M., 2001, *MNRAS*, 326, 1517

¹⁰ The sphere-of-influence is the region of space within which the gravitational potential of the black hole dominates over that of the surrounding stars.

- Dotti M., Montuori C., Decarli R., Volonteri M., Colpi M., Haardt F., 2009, *MNRAS*, 398, L73
- Dotti M., Sesana A., Decarli R., 2012, *Advances in Astronomy*, 2012
- Dullo B. T., Graham A. W., 2014, *MNRAS*, 444, 2700
- Elmegreen D. M., Chromey F. R., Johnson C. O., 1995, *AJ*, 110, 2102
- Emsellem E., 2013, *MNRAS*, 433, 1862
- Emsellem E. et al., 2011, *MNRAS*, 414, 888
- Emsellem E. et al., 2008, in *IAU Symposium*, Vol. 245, *IAU Symposium*, Bureau M., Athanassoula E., Barbu B., eds., pp. 11–14
- Erwin P., Debattista V. P., 2013, *MNRAS*, 431, 3060
- Fabbiano G., Wang J., Elvis M., Risaliti G., 2011, *Nature*, 477, 431
- Favata M., Hughes S. A., Holz D. E., 2004, *ApJ*, 607, L5
- Ferrarese L. et al., 2006, *ApJS*, 164, 334
- Ferrarese L., Ford H., 2005, *Space Sci. Rev.*, 116, 523
- Ferrarese L., Merritt D., 2000, *ApJ*, 539, L9
- Fitchett M. J., Detweiler S., 1984, *MNRAS*, 211, 933
- Fraser-McKelvie A., Brown M. J. I., Pimbblet K. A., 2014, *ArXiv e-prints*
- Gavazzi G., Boselli A., Donati A., Franzetti P., Scodreggio M., 2003, *A&A*, 400, 451
- Gebhardt K. et al., 2000, *ApJ*, 539, L13
- Gebhardt K. et al., 2007, *ApJ*, 671, 1321
- Graham A., 2007, in *Bulletin of the American Astronomical Society*, Vol. 39, *American Astronomical Society Meeting Abstracts*, p. 759
- Graham A. W., 2004, *ApJ*, 613, L33
- Graham A. W., 2008a, *ApJ*, 680, 143
- Graham A. W., 2008b, *PASA*, 25, 167
- Graham A. W., 2012, *ApJ*, 746, 113
- Graham A. W., Erwin P., Trujillo I., Asensio Ramos A., 2003, *AJ*, 125, 2951
- Graham A. W., Li I.-h., 2009, *ApJ*, 698, 812
- Graham A. W., Onken C. A., Athanassoula E., Combes F., 2011, *MNRAS*, 412, 2211
- Graham A. W., Scott N., 2013, *ApJ*, 764, 151
- Graham A. W., Spitler L. R., 2009, *MNRAS*, 397, 2148
- Greenhill L. J. et al., 2003, *ApJ*, 590, 162
- Gualandris A., Merritt D., 2008, *ApJ*, 678, 780
- Gutiérrez L., Erwin P., Aladro R., Beckman J. E., 2011, *AJ*, 142, 145
- Haines C. P. et al., 2013, *ApJ*, 775, 126
- Hartmann M., Debattista V. P., Cole D. R., Valluri M., Widrow L. M., Shen J., 2013, *ArXiv e-prints*
- Hirschmann M., Khochfar S., Burkert A., Naab T., Genel S., Somerville R. S., 2010, *MNRAS*, 407, 1016
- Holley-Bockelmann K., Gültekin K., Shoemaker D., Yunes N., 2008, *ApJ*, 686, 829
- Houghton R. C. W., Magorrian J., Sarzi M., Thatte N., Davies R. L., Krajnović D., 2006, *MNRAS*, 367, 2
- Hu J., 2008, *MNRAS*, 386, 2242
- Hyde J. B., Bernardi M., Sheth R. K., Nichol R. C., 2008, *MNRAS*, 391, 1559
- Jahnke K., Macciò A. V., 2011, *ApJ*, 734, 92
- Jeong H., Bureau M., Yi S. K., Krajnović D., Davies R. L., 2007, *MNRAS*, 376, 1021
- Ju W., Greene J. E., Rafikov R. R., Bickerton S. J., Badenes C., 2013, *ApJ*, 777, 44
- Komossa S., Burwitz V., Hasinger G., Predehl P., Kaastra J. S., Ikebe Y., 2003, *ApJ*, 582, L15
- Kormendy J., Bender R., Cornell M. E., 2011, *Nature*, 469, 374
- Lauer T. R. et al., 2007, *ApJ*, 662, 808
- Laurikainen E., Salo H., Buta R., Knapen J. H., Comerón S., 2010, *MNRAS*, 405, 1089
- Lena D., Robinson A., Marconi A., Axon D. J., Capetti A., Merritt D., Batcheldor D., 2014, *ArXiv e-prints*
- Liu F. S., Xia X. Y., Mao S., Wu H., Deng Z. G., 2008, *MNRAS*, 385, 23
- Liu X., Shen Y., Bian F., Loeb A., Tremaine S., 2014, *ApJ*, 789, 140
- Malumuth E. M., Kirshner R. P., 1981, *ApJ*, 251, 508
- Maness H. L., Taylor G. B., Zavala R. T., Peck A. B., Pollack L. K., 2004, *ApJ*, 602, 123
- Mazzalay X. et al., 2014, *MNRAS*, 438, 2036
- McConnell N. J., Ma C.-P., 2013, *ApJ*, 764, 184
- McNeil-Moylan E. K., Freeman K. C., Arnaboldi M., Gerhard O. E., 2012, *A&A*, 539, A11
- Merritt D., 2006a, *Reports on Progress in Physics*, 69, 2513
- Merritt D., 2006b, *ApJ*, 648, 976
- Merritt D., 2013a, *Dynamics and Evolution of Galactic Nuclei*
- Merritt D., 2013b, *Classical and Quantum Gravity*, 30, 244005
- Merritt D., Ferrarese L., 2001a, in *Astronomical Society of the Pacific Conference Series*, Vol. 249, *The Central Kiloparsec of Starbursts and AGN: The La Palma Connection*, Knapen J. H., Beckman J. E., Shlosman I., Mahoney T. J., eds., p. 335
- Merritt D., Ferrarese L., 2001b, *ApJ*, 547, 140
- Merritt D., Milosavljević M., Favata M., Hughes S. A., Holz D. E., 2004, *ApJ*, 607, L9
- Milosavljević M., Merritt D., 2001, *ApJ*, 563, 34
- Moellenhoff C., Matthias M., Gerhard O. E., 1995, *A&A*, 301, 359
- Morrison H., Caldwell N., Schiavon R. P., Athanassoula E., Romanowsky A. J., Harding P., 2011, *ApJ*, 726, L9
- Naab T., Johansson P. H., Ostriker J. P., 2009, *ApJ*, 699, L178
- Nipoti C., Londrillo P., Ciotti L., 2003, *MNRAS*, 342, 501
- Peng C. Y., 2007, *ApJ*, 671, 1098
- Redmount I. H., Rees M. J., 1989, *Comments on Astrophysics*, 14, 165
- Rodriguez C., Taylor G. B., Zavala R. T., Peck A. B., Pollack L. K., Romani R. W., 2006, *ApJ*, 646, 49
- Rusli S. P., Erwin P., Saglia R. P., Thomas J., Fabricius M., Bender R., Nowak N., 2013a, *AJ*, 146, 160
- Rusli S. P. et al., 2013b, *AJ*, 146, 45
- Sani E., Marconi A., Hunt L. K., Risaliti G., 2011, *MNRAS*, 413, 1479
- Schechter P. L., 1980, *AJ*, 85, 801
- Scott N., Davies R. L., Houghton R. C. W., Cappellari M., Graham A. W., Pimbblet K. A., 2014, *MNRAS*, 441, 274
- Scott N., Graham A. W., Schombert J., 2013, *ApJ*, 768, 76
- Sillanpää A., Haarala S., Valtonen M. J., Sundelius B., Byrd G. G., 1988, *ApJ*, 325, 628
- Thomas J., Saglia R. P., Bender R., Erwin P., Fabricius M., 2014, *ApJ*, 782, 39
- Trujillo I., Erwin P., Asensio Ramos A., Graham A. W., 2004, *AJ*, 127, 1917

- Valluri M., Merritt D., Emsellem E., 2004, ApJ, 602, 66
van den Bosch R. C. E., Gebhardt K., Gültekin K., van de
Ven G., van der Wel A., Walsh J. L., 2012, Nature, 491,
729
Volonteri M., Ciotti L., 2013, ApJ, 768, 29
von der Linden A., Best P. N., Kauffmann G., White
S. D. M., 2007, MNRAS, 379, 867